Chem

CellPress

Article

# A Star of David [2]catenane of single handedness

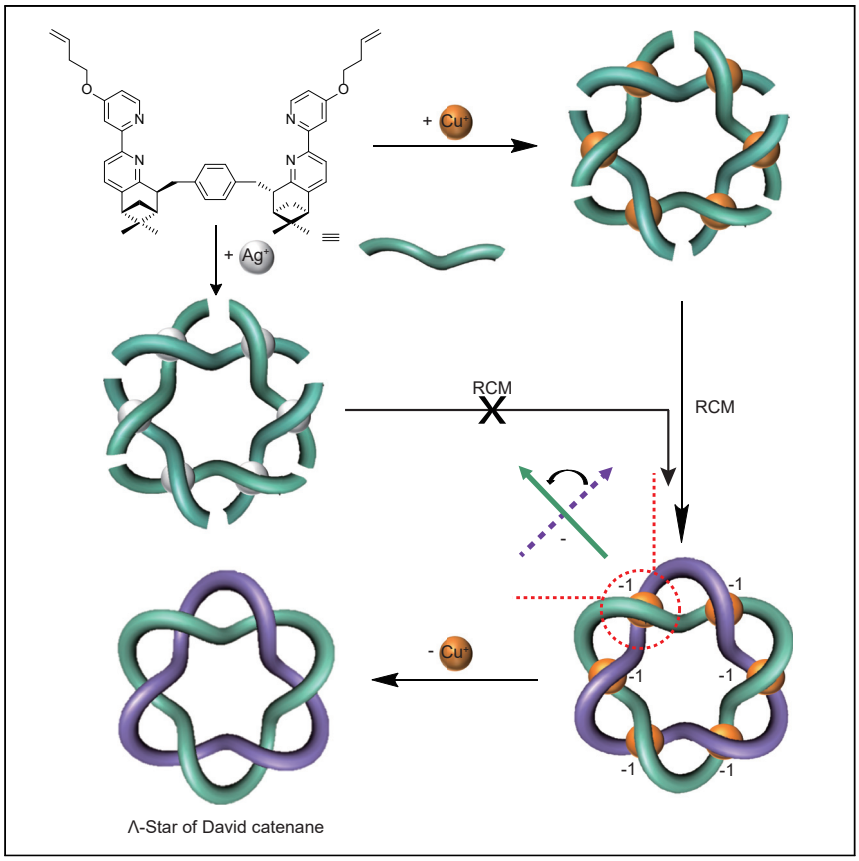


Efficient synthesis of topologically chiral links with controlled handedness is challenging, despite several molecular prime links that have been prepared. Here, we described the two-step highly stereoselective synthesis of a Star of David [2] catenane ( $6_1^2$). Use of CHIRAGENs containing chiral centers closed to coordination sites allows the transfer of the point chirality of the ligands to the topological chirality of the resulting link. This study opens the way to explore the development and potential of topological stereochemistry in chemistry and beyond.

Hai-Na Feng, Zhanhu Sun, Sujun Chen, ..., Tu Sun, Yanhang Ma, Liang Zhang

zhangliang@chem.ecnu.edu.cn

## Highlights

Two-step stereoselective synthesis of a Star of David [2] catenane ($6_1^2$) is achieved

Topological writhe of the link is predetermined by the configuration of ligand

The catenand shows weaker CD response than that of the ligand and macrocycle

Feng et al., Chem 9, 859–868
April 13, 2023 © 2022 Elsevier Inc.
https://doi.org/10.1016/j.chempr.2022.11.010

Chem

CellPress

Article

# A Star of David [2]catenane of single handedness

Hai-Na Feng,[1,6] Zhanhu Sun,[1,6] Sujun Chen,[1] Zhi-Hui Zhang,[1] Zhiming Li,[2] Zhiye Zhong,[3] Tu Sun,[3] Yanhang Ma,[3,4] and Liang Zhang[1,5,7,*]

## SUMMARY

**Prime links with multiple interlocked components feature unconditional topological chirality. Although several prime links have been constructed to date, the control of their chirality with high stereoinduction is rare. Here, we report the stereoselective synthesis of an iconic molecular $6_1^2$ link (Star of David [2]catenane) comprising two triply entwined 84-membered rings. The single-handed Star of David catenane is generated from the closure of a hexameric copper(I) circular helicate by ring-closing olefin metathesis, and the topological writhe ($w = -6$) was predetermined by the configuration of the chiral ligand. Conformation of the topology was proven through NMR spectroscopy and mass spectrometry, whereas the handedness of the link was further investigated through circular dichroism. Stereoselective synthesis of molecular nanotopologies with certain topological writhe by chiral information transfer opens the way to probe the consequences and potential of topological stereochemistry in chemistry, materials, and biology.**

## INTRODUCTION

Links (generally termed "catenanes" in molecular systems)[1] are a collection of structures formed by mechanically interlocked closed loops (macrocycles). Complex molecular links are found in DNA[2,3] and proteins.[4,5] The unique geometry and dynamics of links can be exploited in functional materials[6,7] and artificial molecular machinery.[8] Molecular links are either conditionally topologically chiral[9] or unconditionally topologically chiral.[10] Despite several synthetic strategies to molecular prime links with different topologies have been discovered,[11–15] the stereoselective synthesis of topologically chiral links with controlled handedness is mainly limited to the simplest Hopf link[9,16–29] ($2_1^2$) (Figure 1A) and metallalinks.[30–32] The early remarkable example of enantioselective preparation of a topologically chiral Solomon link ( $4_1^2$, doubly interlocked [2]catenane) was disclosed by Sanders and co-workers.[33] The organic link was obtained as a single topological stereoisomer from a dynamic combinatorial library containing chiral building blocks.

Multimetal-ion circular helicates have been proved to be effective scaffolds for assembly of a series of nanotopologies[34,35] by regulating the shape, size, and strand connectivity.[36–39] Since all metal centers feature same stereochemistry within the helicate (all Λ or Δ), it is obvious that both the helical chirality of the intermediate helicate and the topologically chirality of resulted topology are directly determined by the absolute configuration of the metal centers. A family of pyridine and bipyridine ligands with appended stereogenic centers developed by von Zelewsky and coworkers[40] has been termed chirality generators (CHIRAGENs) because these stereogenic centers can induce the chirality at metal coordination site in a highly stereoselective manner.[41,42] Application of chirality transfer in metal-template synthesis

## THE BIGGER PICTURE

A plethora of strategies have been developed for the construction of molecular links since 1960; however, the highly stereoselective synthesis of inherently chiral links is still challenging. A two-step stereoselective preparation of a topologically chiral $6_1^2$ link, in the shape of a Star of David, is presented. Six equivalent of metal-ion templates is employed to drive self-assembly with six chiral building blocks into a helicate scaffold; a suitable bridge is designed between two chelating sites to direct the size of this hexamer; the length and conformational freedom of extended aliphatic olefin chains are modeled to ensure successful metathesis toward the desired connectivity; and the chiral moiety adjacent to the coordination units is placed to secure topological chirality. Such tactics are practically important in molecular nanotopology and create opportunities not only to explore the effects of chemical constitution on topological and tangled materials but also to elucidate the consequences of topological chirality in chemistry and beyond.

enables to not only render amphicheiral (topologically achiral in 3D) Borromean rings chiral[43] but also prepare topological chiral molecular knots of single handedness.[44–47] Accordingly, if one link is unconditionally topologically chiral, this tactic should also proceed completely stereoselectivity with only one of the two different topological enantiomers being obtained.

An iconic topology, Star of David [2]catenane ($6_1^2$ link in Alexander-Briggs notation[48]) containing two triply interlocked macrocycles is unconditionally topologically chiral (Figure 1A). Leigh and co-workers reported the elegant synthesis by covalent capture of Lehn-type hexameric circular helicate,[49] and the inherently chiral links are formed as racemate by using the achiral tris-bipyridine ligand strand.[50] Although the enantioselective synthesis was achieved later by using a heterometallic helicate, the introduction of unremovable iridium(III) template afforded a metallic link in which the ring dynamic was sacrificed.[51] Different from Lehn-type helicates[49] which are hard to be functionalized, the introduction of well-developed CHIRAGENs[41,42] may provide a general and efficient method in the construction of high-order knots and links with controlled chirality. The early example by von Zelewsky and co-workers presented a highly stereoselective self-assembly of a hexameric circular helicate by using pinene-bipyridine ligand (Figure 1B). Both hexamer and tetramer were detected in solution using silver(I) template,[52,53] whereas only hexamer was formed with copper(I) metal ions.[54] We envisage that this helicate provides an orderly hexagonal entanglement arrangement required for the formation of a Star of David catenane, the suitable alteration of this CHIRAGEN ligand would deliver the construction of the only Λ-enantiomer of a $6_1^2$ link.

## RESULTS AND DISCUSSION

### Highly stereoselective self-assembly of hexameric circular helicate

The ligand frame consists of two pinene-2,2′-bipyridine units connected through a xylene bridge. Molecular modeling suggested that a five-atom chain attached to the 4-position of the pinene-bipyridine moiety, i.e., **1**, should provide the suitable orientation and positioning to promote joining of the ligand strands with desired connectivity (Figure 1B). The chain ends with an alkene so that the ligands can be fused through ring-closing olefin metathesis (RCM), and the metal templates can be subsequently removed to leave a wholly organic catenand.

Chiral ligand **1** was synthesized in six steps from commercially available materials (supplemental information section "synthesis of ligand 1"). Brief stirring of **1** with an equimolar amount of $AgPF_6$ in acetonitrile/chloroform (5:1) at room temperature for 30 min followed by the removal of solvent resulted in a white solid (Figure 2, step i). The $^1$H NMR spectrum (Figure 3B) of the product shows all the ligands to be in equivalent environments. Together with the significant upfield displacement of $H^a$, $H^b$ (1.42 ppm) and $H^{10}$ (0.35 ppm), this indicated the formation of a highly symmetric circular helicate structure. It is worth to mention that neither broadening at 298 K nor splitting at 233 K of $H^a$ and $H^b$ signals was observed (Figure S1) comparing with the previous report,[52] the results suggest the existence of only one type of helicate after introducing the electron-donating group within **1**, rather than two (tetrameric and hexameric circular helicates) rapidly exchanged species. The size of the helicate was further determined by electrospray ionization-mass spectrometry (ESI-MS). Despite the labile nature of silver(I) complexes, weak intensity of *m/z* peaks confirmed it to be the hexamer Λ-$[Ag_6\mathbf{1}_6](PF_6)_6$ (Figure S2).[53] Replacement of $AgPF_6$ with $Cu(MeCN)_4PF_6$ afforded a reddish solid under same condition (Figure 2, step ii), which was characterized as Λ-$[Cu_6\mathbf{1}_6](PF_6)_6$ by ESI-MS (Figure S4) and $^1$H NMR (Figure 3C). There is virtually no circular dichroism (CD) signal of

[1]Shanghai Frontiers Science Center of Molecular Intelligent Synthesis, School of Chemistry and Molecular Engineering, East China Normal University, Shanghai 200062, China

[2]Department of Chemistry, Fudan University, 2005 Songhu Road, Shanghai 200438, China

[3]School of Physical Science and Technology, ShanghaiTech University, Shanghai 201210, China

[4]Shanghai Key Laboratory of High-resolution Electron Microscopy, ShanghaiTech University, Shanghai 201210, China

[5]School of Chemistry and Molecular Engineering, East China Normal University, Shanghai 200062, China

[6]These authors contributed equally

[7]Lead contact

*Correspondence: zhangliang@chem.ecnu.edu.cn

https://doi.org/10.1016/j.chempr.2022.11.010

A

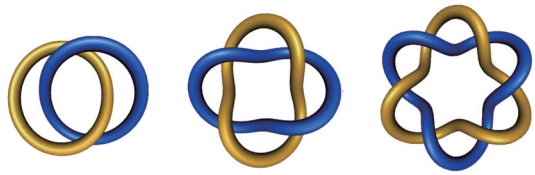

| Topology | Hopf link ($2_1^2$) Interlocked | Solomon link ($4_1^2$) Doubly interlocked | Star of David [2]catenane ($6_1^2$) Triply interlocked |
|---|---|---|---|
| Number of crossings | 2 | 4 | 6 |
| Topological chirality | Conditional | Unconditional | Unconditional |
| Stereoselective synthesis | 12 examples | 2 examples | 1 example |

B

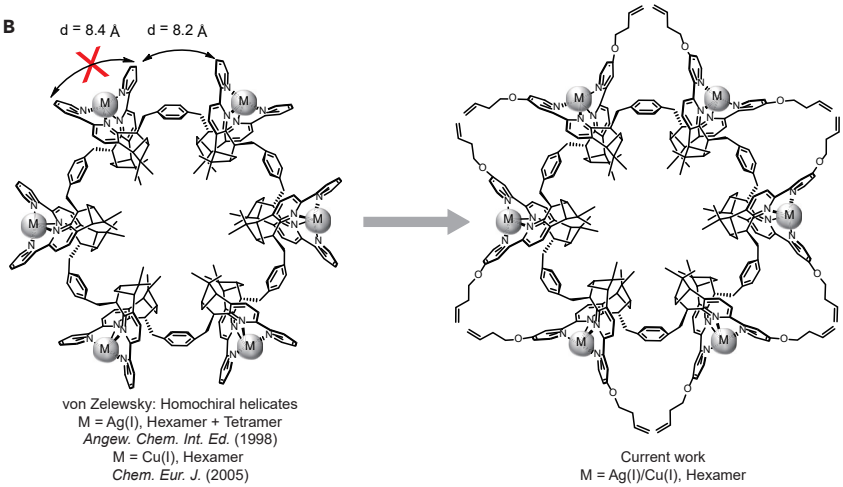


**Figure 1. Difference between three types of braided [2]catenane: the Hopf link ($2_1^2$), the Solomon link( $4_1^2$), and the Star of David catenane ($6_1^2$) and the template synthesis of a Star of David catenane of single handedness from a hexameric circular helicate with the CHIRAGEN ligand**

(A) The cartoon representation of Hopf link, Solomon link, and Star of David catenane. All three catenanes contain two macrocycles but the rings are entwined with each other in different manner, generating different topologies. The Hopf link is conditionally topologically chiral, whereas both Solomon link and Star of David catenane are unconditionally topologically chiral.

(B) The design strategy for the generation of a Star of David catenane of single handedness based on the von Zelewsky's homochiral hexameric helicate framework. The necessary connections between crossings are directed by introducing a suitable chain at the 4-position of the pinene-bipyridine unit, ring-closing olefin metathesis (RCM) joins the chain ends in robust C=C bonds, allowing the metal templates to subsequently be removed to leave a wholly organic entangled $6_1^2$ link. The handedness of the resulting link is predetermined by the handedness of the stereogenic carbon centers in the CHIRAGEN ligand.

ligand **1** in the π-π* (240–320 nm) region of the spectra, obvious CD activity, however, arising from exciton coupling of both helicates (Λ-[$Ag_6$**1**$_6$]$(PF_6)_6$, $\Delta\varepsilon_{245\ nm}$ = +2.0 × $10^6$ $M^{-1}cm^{-1}$ and Λ-[$Cu_6$**1**$_6$]$(PF_6)_6$, $\Delta\varepsilon_{245\ nm}$ = +0.7 × $10^6$ $M^{-1}cm^{-1}$) could be observed (Figure S18). By comparing with the previous results, we reasoned that the point chirality of the ligand has been effectively transferred into the coordinating complex, and it resulted in an enantiomeric circular helicate with all metal centers featuring Λ-configuration.[52–55] The obtained metallic helicates containing regular hexagonal entanglements should be ideal building blocks for the construction of molecular woven materials[56–58] with regular Kagome pattern[59] by having sufficient control of intermolecular connections.

## Formation of Star of David [2]catenate via covalent capture

Ring closure of Λ-[$Ag_6$**1**$_6$]$(PF_6)_6$ in the presence of Hoveyda-Grubbs 2$^{nd}$ catalyst[60] was proven to be unsuccessful under several conditions, probably due to the

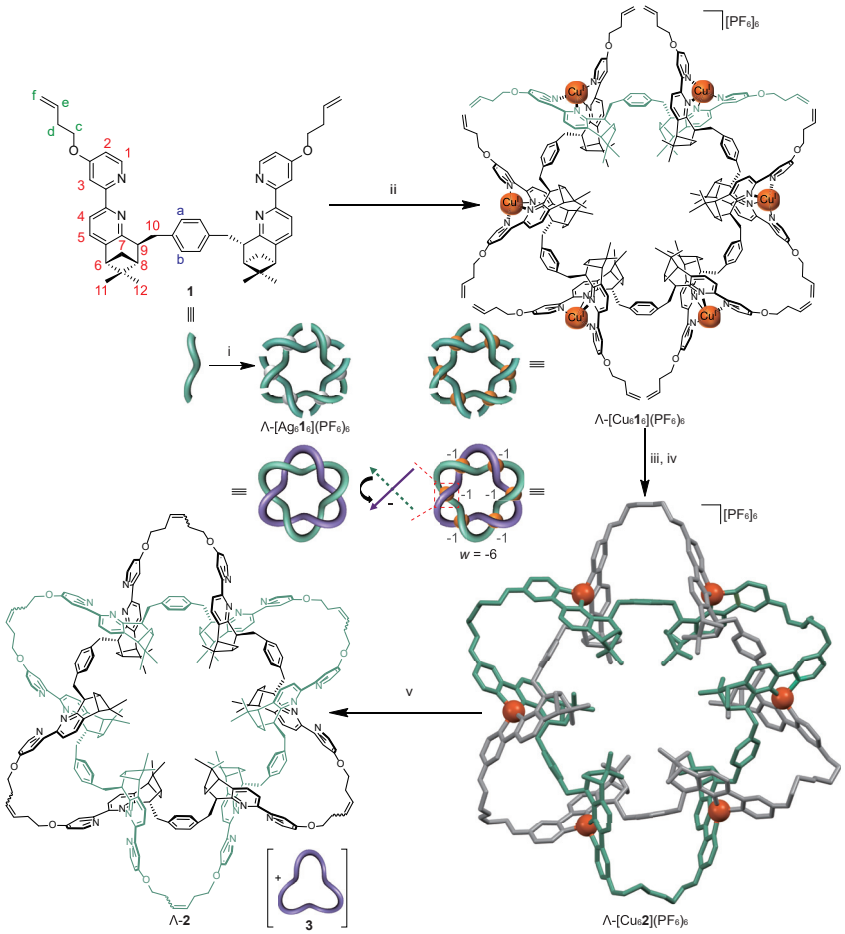


**Figure 2. Completely stereoselective assembly of hexameric circular helicates Λ-[Ag$_6$1$_6$](PF$_6$)$_6$ and Λ-[Cu$_6$1$_6$](PF$_6$)$_6$ and synthesis of homochiral Star of David [2]catenand Λ-2**

All metal centers within Star of David [2]catenate feature only Λ-configuration, which results in the link with negative crossings and −6 topological writhe. The copper(I) Star of David [2]catenate is shown as a simulated model based on the crystal structure of hexameric circular helicate[52] (supplemental information section "density functional theory (DFT) calculations of Λ-[Cu$_6$2](PF$_6$)$_6$" and Table S2). Reaction conditions: (i) $AgPF_6$, $CH_3CN/CHCl_3$ (5:1), room temperature, 30 min, quantitative yield; (ii) $Cu(MeCN)_4PF_6$, $CH_3CN/CHCl_3$ (5:1), room temperature, 30 min, 98% yield; (iii) Hoveyda-Grubbs 2$^{nd}$ catalyst (17 mol % per ligand), $ClCH_2CH_2Cl/MeNO_2$ (1:1), 60°C, 24 h; (iv) excess saturated $KPF_6$ in methanol, 87% yield with around 10%–15% impurity (over two steps); (v) $Na_4EDTA(aq)/CH_3CN$ (1:1), 80°C, 12 h, resulting in Λ-**2** (50%) and **3** (20%).

sensitivity of silver complex toward chloride-substituted ruthenium catalyst. In contrast, subjecting Λ-[Cu$_6$**1**$_6$](PF$_6$)$_6$ to RCM condition, followed by anion exchange with methanolic $KPF_6$ (Figure 2, steps iii and iv) produced the metallated Star of David [2]catenate Λ-[Cu$_6$**2**](PF$_6$)$_6$ (a catenane-metal complex is termed a "catenate" and the interlocked metal-free ligand is a catenand,[61] a simulated model of resulted copper(I)-[2]catenate was shown in Figures 2 and S19). ESI-MS indicated characteristic distributions of *m/z* peaks on account of the loss of corresponding $PF_6^-$ after losing six ethene molecules of the Λ-[Cu$_6$**2**](PF$_6$)$_6$ (Figures S6–S8). The "catenand effect[62]" improved the stability of resulted copper(I) link and gave significantly increased MS peak intensity (Figure S5). The $^1$H NMR spectrum (Figure 3D) also confirmed the absence of terminal alkene protons and the presence of a broad signal at 5.63 ppm for the internal alkene H$^e$ protons. Small amount of polymeric

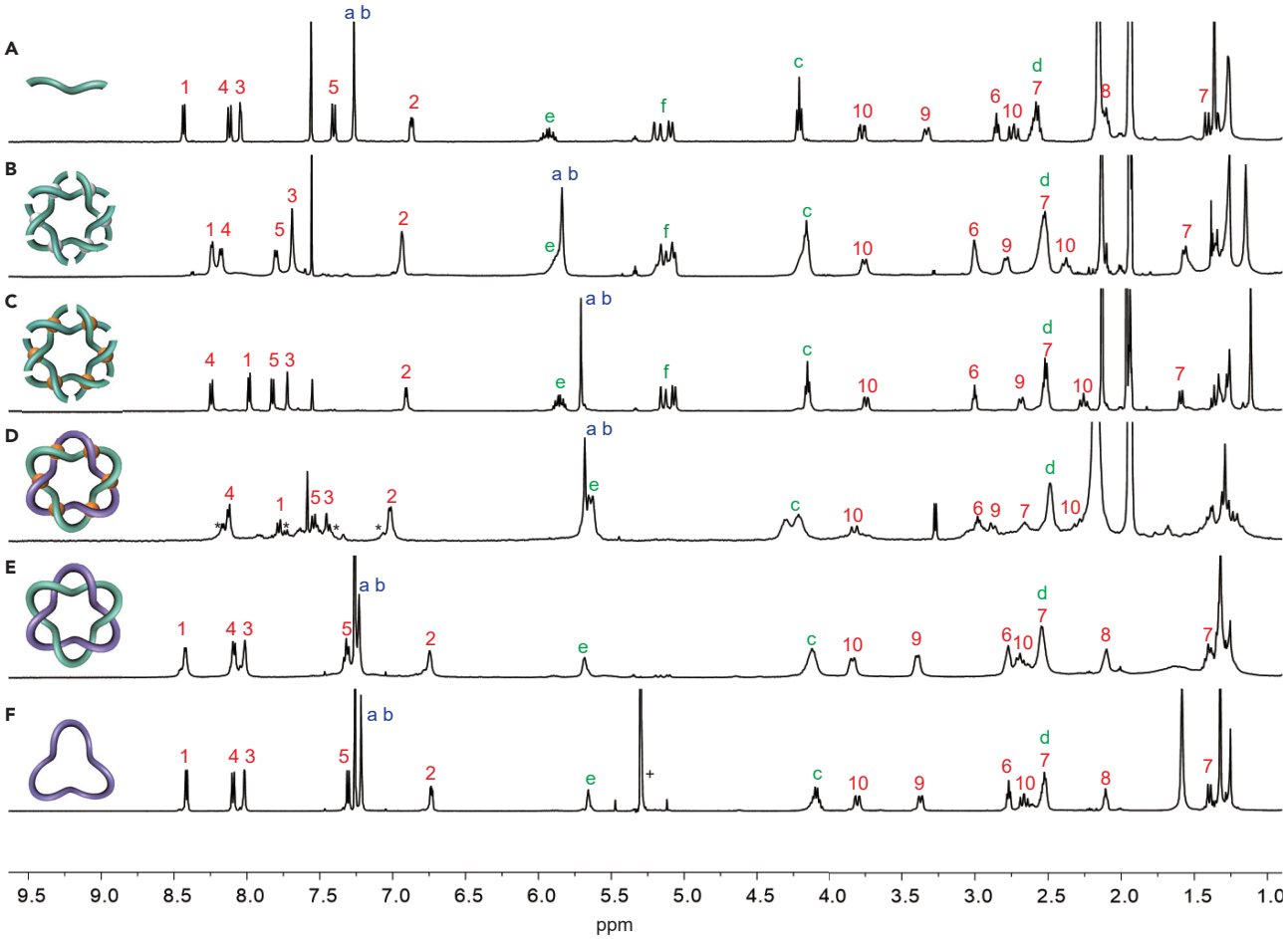


**Figure 3. $^{1}$H NMR spectra (500 MHz, 298 K) of ligand strand (1), hexameric circular helicates (Λ-[M$_6$**1**$_6$](PF$_6$)$_6$ (M = Cu(I) or Ag(I)), metallated (Λ-[Cu$_6$2](PF$_6$)$_6$) and demetallated Star of David [2]catenane (Λ-2) and unlinked macrocycle (3)**

(A) Ligand strand **1** (solvent $CD_3CN/CDCl_3$ (5:1)).

(B) Hexameric circular helicate Λ-[Ag$_6$**1**$_6$](PF$_6$)$_6$ (solvent $CD_3CN/CDCl_3$ (5:1)).

(C) Hexameric circular helicate Λ-[Cu$_6$**1**$_6$](PF$_6$)$_6$ (solvent $CD_3CN/CDCl_3$ (5:1)).

(D) Star of David [2]catenate Λ-[Cu$_6$**2**](PF$_6$)$_6$ (solvent $CD_3CN/CDCl_3$ (5:1)), minor impurity (~10%–15% according to $^{1}$H NMR integration) was obtained during the RCM and could not be removed by conventional separation processes. The impurity is labeled with *.

(E) Star of David [2]catenand Λ-**2** (solvent $CDCl_3$).

(F) Unlinked macrocycle **3** (solvent $CDCl_3$), $^{+}CH_2Cl_2$. The signal assignments correspond to the labeling shown in Figure 2.

by-product (around 10%–15% according to $^{1}$H NMR integration) was formed and could not be removed from the metallic link through conventional purification process (e.g., re-crystallization, anion exchange, and solvent wash), which is probably due to the decomposition, followed by polymerization of the labile copper(I) helicate under RCM condition.

The topological writhe (*w*, also called Tait number[63]) of a link (knots could be considered special cases of links with one component) is the sum of all signs of its crossing points in a standard projection (projection of the link without nugatory crossing).[64] The obtained number depends only on the link type and is thus a topological invariant of a link. Since only left-handed crossings were generated through chiral transformation, the topological writhe of the resulted [2]catenate was scored as −6 (Figure 2). The value is directly determined by the configuration of the asymmetric carbon centers within ligand strand **1**. Despite crucial applications of writhe

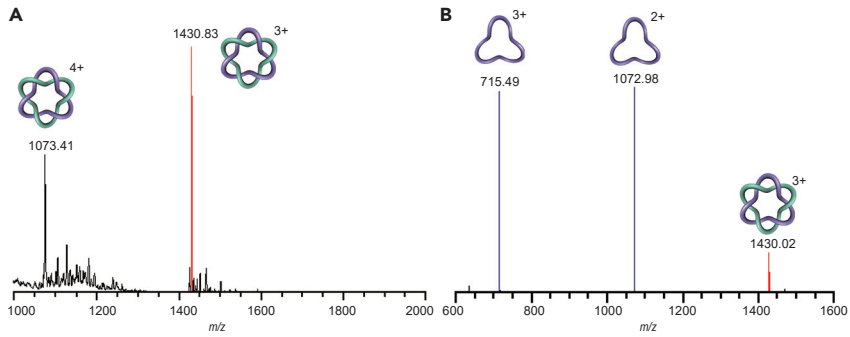


**Figure 4. Low-resolution (LR) ESI-MS characterization and MS/MS experiment on Star of David [2]catenand Λ-2**

(A) ESI-MS of demetallated Star of David [2]catenand Λ-**2** with formic acid added to generate multiply protonated ions. Calculated peaks (*m/z*) = 1,430.79 $[M+3H]^{3+}$, 1,073.10 $[M+4H]^{4+}$.

(B) Tandem mass spectrometry of the $[M+3H]^{3+}$ peak (*m/z* = 1,430.83) from Λ-**2**, which demonstrates the formation of a macrocycle (*m/z* = 1,072.98, calculated $[M+2H]^{2+}$ 1,073.10, *m/z* = 715.49, calculated $[M+3H]^{3+}$ 715.73) from the fragmentation of [2]catanand.

in knot theory and DNA,[65–68] the implications of writhe on small-molecule systems are yet to be realized.[38] The stereoselective synthesis of small molecular topologies with specific topological writhe may deliver a potential strategy to elucidate the mechanisms of such fundamental process in nature.

## Wholly organic Star of David [2]catenand

The [2]catenate was demetallated by treatment of an acetonitrile solution of Λ-$[Cu_6\mathbf{2}](PF_6)_6$ with aqueous tetrasodium ethylenediaminetetraacetate ($Na_4EDTA$) (Figure 2, step v). The color of the solution changed from reddish brown to beige after 30 min, implying the successful removal of copper(I) templates. Two products were isolated by size exclusion chromatography (SEC). The major product (50%) was characterized as the organic Star of David [2]catenand Λ-**2** (Figures 4A and S9), whereas the minor product (20%), which has a molecular mass equal to half that of Λ-**2** (Figure S12), was assigned to be the unlinked macrocycle **3**. The formation of macrocycle could be attributed to either the decomposition of labile copper(I) helicate during ring closure or the opening of Λ-**2** triggered by the trace amount of ruthenium species from the ring-closure reaction.[50] The $^1$H NMR spectra of Λ-**2** and **3** are very similar (Figures 3E and 3F), suggesting that the triply entwined macrocycles within the link feature similar chemical environment as the unlinked macrocycle in solution. This could be attributed to the relatively loose conformation and the fast reptation[69] of ring components within the [2]catenand. Variable-temperature $^1$H NMR spectra of Λ-**2** shows little change over the temperature range (243–323 K) which further supports our hypothesis (Figure S33). The diffusion-ordered spectroscopy NMR (DOSY) showed that Λ-**2** ($D = 1.2 \times 10^{-10}$ $m^2s^{-1}$) and **3** ($D = 6.0 \times 10^{-10}$ $m^2s^{-1}$) process different diffusion coefficient (Figures S32 and S37). The interlocked architecture of the [2]catenand was clearly confirmed by tandem mass spectrometry experiments (MS/MS). The parent $[\Lambda\text{-}\mathbf{2}+3H]^{3+}$ ion at *m/z* 1,430.83 was activated by collision induced dissociation, which resulted in multiple charged ions that originate from the link. Two peaks at *m/z* 715.49 ($[M+3H]^{3+}$) and 1,072.98 ($[M+2H]^{2+}$) were detected, corresponding to a structure with half mass of the [2]catanand (Figure 4B). The results are consistent with the typical fragmentation process of a [2]catenand[70] which breaks one macrocycle and causes the dethreading to form a single ring that remains charged.

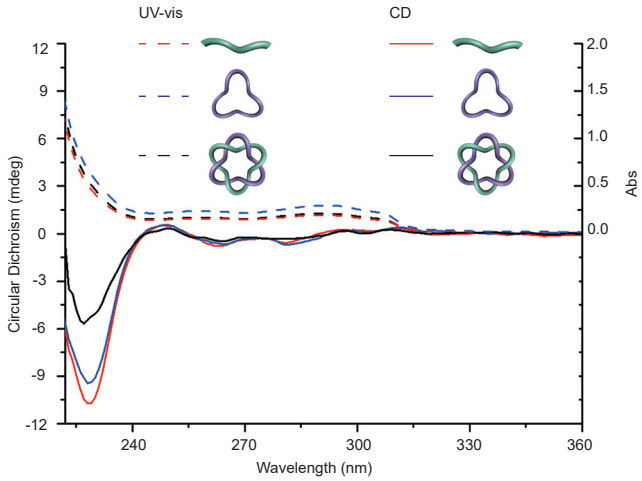


**Figure 5. Overlay of the UV-vis and CD spectra ($CH_2Cl_2$, 298 K) of ligand strand 1 ($6.0 \times 10^{-5}$ M), unlinked macrocycle 3 ($2.0 \times 10^{-5}$ M) and link Λ-2 ($1.0 \times 10^{-5}$ M)**

The concentration of ligand and macrocycle were adjusted on account of the number of chromophores and stereogenic carbon centers in each molecule, so that the absorbance intensity and CD response among three compounds can be directly compared. The UV-vis spectra were presented in dash line, and the CD spectra presented in sloid line. **Λ-2** showed much weaker chiral expression than that of ligand and macrocycle in the range of 220–240 nm.

The organic Star of David [2]catenand **Λ-2** is remetallated by treatment with $Cu(MeCN)_4PF_6$ in a dichloromethane/acetonitrile (1:1) mixture at 60°C for 24 h, and the regeneration of the Star of David [2]catenate can be clearly confirmed by both low-resolution (LR)- and high-resolution (HR)-ESI (Figures S14–S16). Although the $^1$H NMR spectrum of the remetallated link is broader than that of the metallated link obtained from ring closure, most of proton signals are in similar chemical shifts (Figure S13). Considering that there are 12 chelating vacancies in the organic link, we assume that the "wrong" combinations between bipyridine units and copper(I) ions are hard to be corrected due to the slow coordination dynamics. Nevertheless, the reformation of the catenate is a further proof of the formation of the Star of David catenane topology.

The synthetic availability allows us to further explore the consequences in properties among the uncoordinated ligand strand, unlinked macrocycle and [2]catenand. To directly probe the differences among three compounds, the concentration of ligand and macrocycle are adjusted ($c_1 = 6 \times c_{\Lambda\text{-}2}$, $c_3 = 2 \times c_{\Lambda\text{-}2}$) by considering the number of chromophores and stereogenic carbon centers in each molecule. The ultraviolet-visible (UV-vis) absorption spectra of ligand **1**, macrocycle **3**, and link **Λ-2** have similar profiles with absorption band at λ = 230 (pyridyl n-$\pi^*$), 257, and 291 nm (bipyridine $\pi$-$\pi^*$) in the expected region for bipyridine units (Figure 5). The similar absorbance intensities indicated the chromophores were in similar environment in different topologies, which again supports the results obtained from $^1$H NMR.

The triply entwined $6_1^2$ link is unconditionally topologically chiral by virtue of its topology. CD spectra of three compounds all displayed negative Cotton effect. The CD response of macrocycle is slightly lower than that of the ligand, but other than this, the spectra of **1** and **3** are similar, both a reflection of the influence of the chiral centers on the adjacent chromophores. The induced CD signal of the catenand **Λ-2**,

however, is noticeably weaker (~0.5×) than that of the ligand and macrocycle in the range 220–240 nm (Figure 5). It should be noted that in the absence of the metal-ion templates, the organic [2]catenand would adapt multiple interconverted dissymmetric and asymmetric conformations through backbone reptation instead of a well-defined $D_6$-helical symmetry, which average out to give the CD responses.[71]

## EXPERIMENTAL PROCEDURES

### Resource availability

*Lead contact*

Liang Zhang, zhangliang@chem.ecnu.edu.cn.

*Materials availability*

This study did not generate new reagents.

*Data and code availability*

The three-dimensional electron diffraction (3D ED) data are included in the supplemental information and the full set of data is available on request from L.Z.

## SUPPLEMENTAL INFORMATION

Supplemental information can be found online at https://doi.org/10.1016/j.chempr.2022.11.010.

## ACKNOWLEDGMENTS

L.Z. thanks the East China Normal University, the Shanghai Frontiers Science Center of Molecular Intelligent Synthesis, the National Natural Science Foundation of China (22001074), the Shanghai Sailing Program (20YF1411400), and the Natural Science Foundation of Shanghai (22ZR1479400) for financial support. S.C. thanks the Postdoctoral Research Foundation of China (22101085) for funding. Y.M. and Z.Z. thank the National Natural Science Foundation of China (22222108), the Shanghai Science and Technology Plan (21DZ2260400), CħEM, the School of Physical Sciences and Technology, and ShanghaiTech University (EM02161943) for funding.

Dedicated to Sir James Fraser Stoddart (Northwest University), a pioneer of *Artificial Molecular Machine* and *Molecular Nanotopology*, on the occasion of his 80th Birthday.

## AUTHOR CONTRIBUTIONS

H.-N.F., Z.S., S.C., and Z.-H.Z. carried out the synthesis and characterization. Z.L. performed the simulation. Z.Z., T.S., and Y.M. conducted electron diffraction and structural analysis. H.-N.F. and Z.S. contributed equally. L.Z. directed the research. All the authors contributed to the analysis of the results and the writing of the manuscript.

## DECLARATION OF INTERESTS

The authors declare no competing interests.

Received: April 25, 2022
Revised: August 15, 2022
Accepted: November 9, 2022
Published: December 5, 2022

## REFERENCES


1. Bruns, C.J., and Stoddart, J.F. (2016). The Nature of the Mechanical Bond: From Molecules to Machines (John Wiley & Sons, Inc).
2. Nitiss, J.L., and Stepanov, A. (2005). DNA topoisomerases. In Encyclopedic Reference of Genomics and Proteomics in Molecular Medicine, D. Ganten, et al. (Springer). https://doi.org/10.1007/3-540-29623-9_2610.
3. Champoux, J.J. (2001). DNA topoisomerases: structure, function, and mechanism. Annu. Rev. Biochem. *70*, 369–413. https://doi.org/10.1146/annurev.biochem.70.1.369.
4. Wikoff, W.R., Liljas, L., Duda, R.L., Tsuruta, H., Hendrix, R.W., and Johnson, J.E. (2000). Topologically linked protein rings in the bacteriophage HK97 capsid. Science *289*, 2129–2133. https://doi.org/10.1126/science.289.5487.2129.
5. Mashaghi, A., van Wijk, R.J., and Tans, S.J. (2014). Circuit topology of proteins and nucleic acids. Structure *22*, 1227–1237. https://doi.org/10.1016/j.str.2014.06.015.
6. Meng, W., Kondo, S., Ito, T., Komatsu, K., Pirillo, J., Hijikata, Y., Ikuhara, Y., Aida, T., and Sato, H. (2021). An elastic metal-organic crystal with a densely catenated backbone. Nature *598*, 298–303. https://doi.org/10.1038/s41586-021-03880-x.
7. Au-Yeung, H.Y., and Deng, Y. (2022). Distinctive features and challenges in catenane chemistry. Chem. Sci. *13*, 3315–3334. https://doi.org/10.1039/D1SC05391D.
8. Zhang, L., Marcos, V., and Leigh, D.A. (2018). Molecular machines with bio-inspired mechanisms. Proc. Natl. Acad. Sci. USA *115*, 9397–9404. https://doi.org/10.1073/pnas.1712788115.
9. Jamieson, E.M.G., Modicom, F., and Goldup, S.M. (2018). Chirality in rotaxanes and catenanes. Chem. Soc. Rev. *47*, 5266–5311. https://doi.org/10.1039/C8CS00097B.
10. Walba, D.M. (1985). Topological stereochemistry. Tetrahedron *41*, 3161–3212. https://doi.org/10.1016/S0040-4020(01)96671-2.
11. Forgan, R.S., Sauvage, J.P., and Stoddart, J.F. (2011). Chemical topology: complex molecular knots, links, and entanglements. Chem. Rev. *111*, 5434–5464.
12. Gil-Ramírez, G., Leigh, D.A., and Stephens, A.J. (2015). Catenanes: fifty years of molecular links. Angew. Chem. Int. Ed. Engl. *54*, 6110–6150. https://doi.org/10.1002/anie.201411619.
13. Cougnon, F.B.L., Caprice, K., Pupier, M., Bauzá, A., and Frontera, A. (2018). A strategy to synthesize molecular knots and links using the hydrophobic effect. J. Am. Chem. Soc. *140*, 12442–12450. https://doi.org/10.1021/jacs.8b05220.
14. Qu, Z., Cheng, S.Z.D., and Zhang, W.-B. (2021). Macromolecular topology engineering. J. Trends Chem. *3*, 402–415. https://doi.org/10.1016/j.trechm.2021.02.002.
15. Schröder, H.V., Zhang, Y., and Link, A.J. (2021). Dynamic covalent self-assembly of mechanically interlocked molecules solely made from peptides. Nat. Chem. *13*, 850–857. https://doi.org/10.1038/s41557-021-00770-7.
16. Mitchell, D.K., and Sauvage, J.-P. (1988). A topologically chiral [2]catenand. Angew. Chem. Int. Ed. Engl. *27*, 930–931. https://doi.org/10.1002/anie.198809301.
17. Armspach, D., Ashton, P.R., Ballardini, R., Balzani, V., Godi, A., Moore, C.P., Prodi, L., Spencer, N., Stoddart, J.F., Tolley, M.S., et al. (1995). Catenated cyclodextrins. Chem. Eur. J. *1*, 33–55. https://doi.org/10.1002/chem.19950010109.
18. Lam, R.T.S., Belenguer, A., Roberts, S.L., Naumann, C., Jarrosson, T., Otto, S., and Sanders, J.K.M. (2005). Amplification of acetylcholine binding catenanes from dynamic combinatorial libraries. Science *308*, 667–669. https://doi.org/10.1126/science.1109999.
19. Theil, A., Mauve, C., Adeline, M.-T., Marinetti, A., and Sauvage, J.-P. (2006). Phosphorus-containing [2]catenanes as an example of interlocking chiral structures. Angew. Chem. Int. Ed. Engl. *45*, 2104–2107. https://doi.org/10.1002/anie.200503625.
20. Chung, M.-K., White, P.S., Lee, S.J., and Gagné, M.R. (2009). Synthesis of interlocked 56-membered rings by dynamic self-templating. Angew. Chem. Int. Ed. Engl. *48*, 8683–8686. https://doi.org/10.1002/anie.200903478.
21. Au-Yeung, H.Y., Dan Pantoş, G.D., and Sanders, J.K.M. (2009). Amplifying different [2]catenanes in an aqueous donor-acceptor dynamic combinatorial library. J. Am. Chem. Soc. *131*, 16030–16032. https://doi.org/10.1021/ja906634h.
22. Au-Yeung, H.Y., Pantos, G.D., and Sanders, J.K.M. (2009). Molecular recognition and self-assembly special feature: Dynamic combinatorial synthesis of a catenane based on donor-acceptor interactions in water. Proc. Natl. Acad. Sci. USA *106*, 10466–10470. https://doi.org/10.1073/pnas.0809934106.
23. Prakasam, T., Lusi, M., Nauha, E., Olsen, J.-C., Sy, M., Platas-Iglesias, C., Charbonnière, L.J., and Trabolsi, A. (2015). Dynamic stereoisomerization in inherently chiral bimetallic [2]catenanes. Chem. Commun. (Camb) *51*, 5840–5843. https://doi.org/10.1039/c4cc07392d.
24. Dehkordi, M.E., Luxami, V., and Pantoş, G.D. (2018). High-yielding synthesis of chiral donor-acceptor catenanes. J. Org. Chem. *83*, 11654–11660. https://doi.org/10.1021/acs.joc.8b01629.
25. Denis, M., Lewis, J.E.M., Modicom, F., and Goldup, S.M. (2019). An auxiliary approach for the stereoselective synthesis of topologically chiral catenanes. Chem *5*, 1512–1520. https://doi.org/10.1016/j.chempr.2019.03.008.
26. Gianga, T.M., Audibert, E., Trandafir, A., Kociok-Köhn, G., and Pantoş, G.D. (2020). Discovery of an all-donor aromatic [2]catenane. Chem. Sci. *11*, 9685–9690. https://doi.org/10.1039/d0sc04317f.
27. Maynard, J.R.J., and Goldup, S.M. (2020). Strategies for the synthesis of enantiopure mechanically chiral molecules. Chem *6*, 1914–1932. https://doi.org/10.1016/j.chempr.2020.07.012.
28. Rodríguez-Rubio, A., Savoini, A., Modicom, F., Butler, P., and Goldup, S.M. (2022). A Co-conformationally "topologically" chiral catenane. J. Am. Chem. Soc. *144*, 11927–11932. https://doi.org/10.1021/jacs.2c02029.
29. Maynard, J.R.J., Gallagher, P., Lozano, D., Butler, P., and Goldup, S.M. (2022). Mechanically axially chiral catenanes and noncanonical mechanically axially chiral rotaxanes. Nat. Chem. *14*, 1038–1044. https://doi.org/10.1038/s41557-022-00973-6.
30. Gao, W.-X., Feng, H.-J., Guo, B.-B., Lu, Y., and Jin, G.-X. (2020). Coordination-directed construction of molecular links. Chem. Rev. *120*, 6288–6325. https://doi.org/10.1021/acs.chemrev.0c00321.
31. Cui, Z., Lu, Y., Gao, X., Feng, H.-J., and Jin, G.-X. (2020). Stereoselective synthesis of a topologically chiral solomon link. J. Am. Chem. Soc. *142*, 13667–13671. https://doi.org/10.1021/jacs.0c05366.
32. Sawada, T., and Fujita, M. (2021). Orderly entangled nanostructures of metal-peptide strands. Bull. Chem. Soc. Jpn. *94*, 2342–2350. https://doi.org/10.1246/bcsj.20210218.
33. Ponnuswamy, N., Cougnon, F.B.L., Pantoş, G.D., and Sanders, J.K.M. (2014). Homochiral and meso figure eight knots and a solomon link. J. Am. Chem. Soc. *136*, 8243–8251. https://doi.org/10.1021/ja4125884.
34. Stoddart, J.F. (2020). Dawning of the age of molecular nanotopology. Nano Lett. *20*, 5597–5600. https://doi.org/10.1021/acs.nanolett.0c02366.
35. Guo, Q.-H., Jiao, Y., Feng, Y., and Stoddart, J.F. (2021). The rise and promise of molecular nanotopology. CCS Chem. *3*, 1542–1572. https://doi.org/10.31635/ccschem.021.202100975.
36. Fielden, S.D.P., Leigh, D.A., and Woltering, S.L. (2017). Molecular knots. Angew. Chem. Int. Ed. Engl. *56*, 11166–11194. https://doi.org/10.1002/anie.201702531.
37. Wood, C.S., Ronson, T.K., Belenguer, A.M., Holstein, J.J., and Nitschke, J.R. (2015). Two-stage directed self-assembly of a cyclic [3]catenane. Nat. Chem. *7*, 354–358. https://doi.org/10.1038/nchem.2205.
38. Zhang, L., Stephens, A.J., Nussbaumer, A.L., Lemonnier, J.-F., Jurček, P., Vitorica-Yrezabal, I.J., and Leigh, D.A. (2018). Stereoselective synthesis of a composite knot with nine crossings. Nat. Chem. *10*, 1083–1088. https://doi.org/10.1038/s41557-018-0124-6.
39. Danon, J.J., Leigh, D.A., Pisano, S., Valero, A., and Vitorica-Yrezabal, I.J. (2018). A six-crossing doubly interlocked [2]catenane with twisted rings, and a molecular granny knot. Angew. Chem. Int. Ed. Engl. *57*, 13833–13837. https://doi.org/10.1002/anie.201807135.
40. von Zelewsky, A., and Mamula, O. (2000). The bright future of stereoselective synthesis of

co-ordination compounds. J. Chem. Soc. Dalton Trans. *3*, 219–231. https://doi.org/10.1039/A908730C.

41. Hayoz, P., von Zelewsky, A., and Stoeckli-Evans, H. (1993). Stereoselective synthesis of octahedral complexes with predetermined helical chirality. J. Am. Chem. Soc. *115*, 5111–5114. https://doi.org/10.1021/ja00065a023.

42. Knof, U., and von Zelewsky, A. (1999). Predetermined chirality at metal centers. Angew. Chem. Int. Ed. Engl. *38*, 302–322. https://doi.org/10.1002/(SICI)1521-3773(19990201)38:3<302::AID-ANIE302>3.0.CO;2-G.

43. Pentecost, C.D., Peters, A.J., Chichak, K.S., Cave, G.W.V., Cantrill, S.J., and Stoddart, J.F. (2006). Chiral borromeates. Angew. Chem. Int. Ed. Engl. *45*, 4099–4104. https://doi.org/10.1002/anie.200600817.

44. Perret-Aebi, L.-E., von Zelewsky, A., Dietrich-Buchecker, C., and Sauvage, J.-P. (2004). Stereoselective synthesis of a topologically chiral molecule: the trefoil knot. Angew. Chem. Int. Ed. Engl. *43*, 4482–4485. https://doi.org/10.1002/anie.200460250.

45. Zhang, G., Gil-Ramírez, G., Markevicius, A., Browne, C., Vitorica-Yrezabal, I.J., and Leigh, D.A. (2015). Lanthanide template synthesis of trefoil knots of single handedness. J. Am. Chem. Soc. *137*, 10437–10442. https://doi.org/10.1021/jacs.5b07069.

46. Zhong, J., Zhang, L., August, D.P., Whitehead, G.F.S., and Leigh, D.A. (2019). Self-sorting assembly of molecular trefoil knots of single handedness. J. Am. Chem. Soc. *141*, 14249–14256. https://doi.org/10.1021/jacs.9b06127.

47. Carpenter, J.P., McTernan, C.T., Greenfield, J.L., Lavendomme, R., Ronson, T.K., and Nitschke, J.R. (2021). Controlling the shape and chirality of an eight-crossing molecular knot. Chem *7*, 1534–1543. https://doi.org/10.1016/j.chempr.2021.03.005.

48. Alexander, J.W., and Briggs, G.B. (1926). On types of knotted curves. Ann. Math. *28*, 562–586. https://doi.org/10.2307/1968399.

49. Hasenknopf, B., Lehn, J., Boumediene, N., Dupont-Gervais, A., Van Dorsselaer, A., Kneisel, B., and Fenske, D. (1997). Self-assembly of tetra- and hexanuclear circular helicates. J. Am. Chem. Soc. *119*, 10956–10962. https://doi.org/10.1021/ja971204r.

50. Leigh, D.A., Pritchard, R.G., and Stephens, A.J. (2014). A Star of David catenane. Nat. Chem. *6*, 978–982. https://doi.org/10.1038/nchem.2056.

51. August, D.P., Jaramillo-Garcia, J., Leigh, D.A., Valero, A., and Vitorica-Yrezabal, I.J. (2021). A chiral cyclometalated iridium Star of David [2]catenane. J. Am. Chem. Soc. *143*, 1154–1161. https://doi.org/10.1021/jacs.0c12038.

52. Mamula, O., von Zelewsky, A., and Bernardinelli, G. (1998). Completely stereospecific self-assembly of a circular helicate. Angew. Chem. Int. Ed. Engl. *37*, 289–293. https://doi.org/10.1002/(SICI)1521-3773(19980216)37:3<289::AID-ANIE289>3.0.CO;2-M.

53. Attempts on analysis of $\Lambda$-[$Ag_6\mathbf{1}_6$]$(PF_6)_6$ in solid state by X-ray diffraction were proven fruitless. Alternatively, three-dimensional electron diffraction (3D ED) was applied on the obtained nanosized crystals of the hexamer helicate. The inherent property-large dimension and huge void space filled with anion and solvent-makes these compounds protein-like and prevent the collection of high-resolution crystal data that is typical for standard metal complexes. The 3D ED data are at a resolution (2.06 Å) that does not allow us to properly completely refine the structure, the simulated model, however, matched with the reconstructed electrostatic potential map (Table S3). Considering the 3D ED has been widely used in solving structures of small-molecule drugs and framework materials, we propose the use of 3D ED characterization combined with structural simulations to determine the specific structure of topologically complex supramolecular architectures. The detail of 3D ED analysis is in supplemental information section "3D ED data collection and crystal structural analysis".

54. Mamula, O., Monlien, F.J., Porquet, A., Hopfgartner, G., Merbach, A.E., and von Zelewsky, A. (2001). Self-assembly of multinuclear coordination species with chiral bipyridine ligands: silver complexes of 5,6-CHIRAGEN(o,m,p-xylidene) ligands and equilibrium behaviour in solution. Chem. Eur. J. *7*, 533–539. https://doi.org/10.1002/1521-3765(20010119)7:2<533::AID-CHEM533>3.0.CO;2-Q.

55. Mamula, O., von Zelewsky, A., Brodard, P., Schläpfer, C.-W., Bernardinelli, G., and Stoeckli-Evans, H. (2005). Helicates of chiragen-type ligands and their aptitude for chiral self-recognition. Chem. Eur. J. *11*, 3049–3057. https://doi.org/10.1002/chem.200401109.

56. Liu, Y., Ma, Y., Zhao, Y., Sun, X., Gándara, F., Furukawa, H., Liu, Z., Zhu, H., Zhu, C., Suenaga, K., et al. (2016). Weaving of organic threads into a crystalline covalent organic framework. Science *351*, 365–369. https://doi.org/10.1126/science.aad4011.

57. August, D.P., Dryfe, R.A.W., Haigh, S.J., Kent, P.R.C., Leigh, D.A., Lemonnier, J.F., Li, Z., Muryn, C.A., Palmer, L.I., Song, Y., et al. (2020). Self-assembly of a layered two-dimensional molecularly woven fabric. Nature *588*, 429–435. https://doi.org/10.1038/s41586-020-3019-9.

58. Zhang, Z.-H., Andreassen, B.J., August, D.P., Leigh, D.A., and Zhang, L. (2022). Molecular weaving. Nat. Mater. *21*, 275–283. https://doi.org/10.1038/s41563-021-01179-w.

59. Lewandowska, U., Zajaczkowski, W., Corra, S., Tanabe, J., Borrmann, R., Benetti, E.M., Stappert, S., Watanabe, K., Ochs, N.A.K., Schaeublin, R., et al. (2017). A triaxial supramolecular weave. Nat. Chem. *9*, 1068–1072. https://doi.org/10.1038/nchem.2823.

60. Garber, S.B., Kingsbury, J.S., Gray, B.L., and Hoveyda, A.H. (2000). Efficient and recyclable monomeric and dendritic Ru-based metathesis catalysts. J. Am. Chem. Soc. *122*, 8168–8179. https://doi.org/10.1021/ja001179g.

61. Sauvage, J.-P. (1990). Interlacing molecular threads on transition metals: catenands, catenates, and knots. Acc. Chem. Res. *23*, 319–327. https://doi.org/10.1021/ar00178a001.

62. Albrecht-Gary, A.M., Saad, Z., Dietrich-Buchecker, C.O., and Sauvage, J.P. (1985). Interlocked macrocyclic ligands: a kinetic catenand effect in copper(I) complexes. J. Am. Chem. Soc. *107*, 3205–3209. https://doi.org/10.1021/ja00297a028.

63. Tait, P.G. (1898). On Knots I II, III in Scientific Papers*I* (Cambridge University Press), pp. 273–347.

64. Cerf, C., and Stasiak, A. (2000). A topological invariant to predict the three-dimensional writhe of ideal configurations of knots and links. Proc. Natl. Acad. Sci. USA *97*, 3795–3798. https://doi.org/10.1073/pnas.97.8.3795.

65. Vinograd, J., and Lebowitz', J. (1966). Physical and topological properties of circular DNA. J. Gen. Physiol. *49*, 103–125. https://doi.org/10.1085/jgp.49.6.103.

66. Cerf, C. (1999). In Ch 1 Chemical Topology: Applications and Techniques, D. Bonchev and D.H. Rouvray, eds. (Gordon and Breach), pp. 1–33.

67. Fogg, J.M., Kolmakova, N., Rees, I., Magonov, S., Hansma, H., Perona, J.J., and Zechiedrich, E.L. (2006). Exploring writhe in supercoiled minicircle DNA. J. Phys. Condens. Matter *18*, S145–S159. https://doi.org/10.1088/0953-8984/18/14/S01.

68. Randall, G.L., Zechiedrich, L., and Pettitt, B.M. (2009). In the absence of writhe, DNA relieves torsional stress with localized, sequence-dependent structural failure to preserve B-form. Nucleic Acids Res. *37*, 5568–5577. https://doi.org/10.1093/nar/gkp556.

69. de Gennes, P.G. (1971). Reptation of a polymer chain in the presence of fixed obstacles. J. Chem. Phys. *55*, 572–579. https://doi.org/10.1063/1.1675789.

70. Vetter, W., and Schill, G. (1967). Die gezielte synthese von catena-verbindungen-IX: das Massenspektrum einer catena-Verbindung. Tetrahedron *23*, 3079–3093. https://doi.org/10.1016/S0040-4020(01)83366-4.

71. Barron, L.D. (2009). In Ch. 1 Chirality at the Nanoscale: Nanoparticles, Surfaces, Materials and More, D.B. Amabilino, ed. (Wiley-VCH Verlag), pp. 1–29. https://doi.org/10.1002/9783527625345.ch1.